

# **Modeling and Optimization of an Autonomous Photovoltaic System Based on Advanced Nonlinear Control**

**Mansori Mohamed\*, Zazi Malika**

Department of electrical engineering  
Higher Normal School of Technical Education  
Mohammed V University  
Rabat, BP 6207, Morocco

[Mohamed.mansori@um5s.net.ma](mailto:Mohamed.mansori@um5s.net.ma) , [m.zazi@um5s.net.ma](mailto:m.zazi@um5s.net.ma)

## **Abstract**

The photovoltaic modules are defined by their current/voltage and power/voltage characteristics which are highly non-linear. These characteristics depend on the climatic conditions and the load, and they admitted one optimum operating point. For this reason, it is necessary to track the maximum power to maximize the PV system efficiency. In this paper, a nonlinear MPPT method based on sliding mode (SMC) is applied to track the maximum power. In this method, the proposed SMC should always calculate the output power of the PV system and optimized it by acting on the duty cycle of the DC/DC converter. To test the robustness of the proposed control strategy, the simulation results are compared with those obtained using the Perturbation and Observation Method (P&O). The comparative studies have shown the effectiveness of the proposed technique against the uncertainties and parameter variation.

**Keywords:** Photovoltaic system, MPPT technique, Sliding mode control, Optimization, DC/DC converter.

## **1. Introduction:**

The use of renewable energies, particularly photovoltaic solar energy, can be a good solution to the growing demand of electricity. This issue does not pollute the atmosphere, avoids nuclear risks and it is independent of fossil fuels that are poorly distributed and exhaustible. However, the photovoltaic conversion is still uncompetitive and presenting important deficiencies in terms of yield and reliability. Therefore, the optimization of the energy transfer in the production chain is very essential to the aim of a fast development of the solar as well. In different studies, it has been demonstrated that the use of static converters piloted by MPPT control improves the conversion efficiency over a wide range of applications.

In the literature, many MPPT techniques have been developed and adapted for tracking the maximum power of a photovoltaic system (PV) [1, 2]. These methods consist of acting on the duty cycle of DC/DC converter to find the voltage at the point of maximum power, and this, whatever the weather conditions and load.

The open circuit voltage method is widely used in the control of a PV system [3], this strategy is based on finding the voltage of the PV generator at the maximum power point (MPP) through the linear approximation of the open-circuit voltage and the voltage at the MPP, the same thing between the current at the MPP with the short-circuit current, as demonstrated in [4]. These methods are simple and economical but they are not able to adapt to climate change.

In [5], the authors present the perturbation and observation method (P&O) which based on the search of MPP through the measurement of the current and voltage of the PV module. It is mostly used due to its simplicity [5, 6], but it presents an undesirable oscillations around the maximum power. The conductance incremental method presented in [6], it is based on the search for the MPP through the search for a zero

derivative of the PV system power. The disadvantage of this command resides in its complexity and instability.

In this paper the technique of sliding mode is applied to track the MPP of PV system. This method presents many advantages, such as a high precision, good stability and fast dynamic response. The algorithm of this command is based on construct of the sliding surface, which represents the point of maximum power. Mostly in SMC, the control law is composed of two control signals: the equivalent component and the discontinuous component. The first one represents the dynamic of the system during the sliding mode and the other represents the dynamic of the system during the convergence mode.

The objective of this work is to contribute to the optimization of a photovoltaic conversion chain. This contribution concerns two main undermentioned points:

- The study of an MPPT method based on a non-linear approach called sliding mode control for the optimal transfer of energy from a PV generator to its load.
- Have a non-isolated DC / DC converter with good efficiency and high voltage gain.

This work is organized as follows: in the section 2, an overall description of the system is briefly presented. The section 3 is dedicated to Modeling of the proposed system. The section 4 is reserved for the application of sliding mode control to track the maximum power of Photovoltaic System .The simulation results and test of robustness of SMC are presented in section 5 and 6. Finally, some conclusions of this work are summarized in section 7.

## 2. Description of the proposed system

The modeling of the photovoltaic system based on power electronic converters remains difficult. This type of structure consist three elements, namely: the primary source of energy (PV panels), the boost converter and the controller system, as depicted in Figure 1.

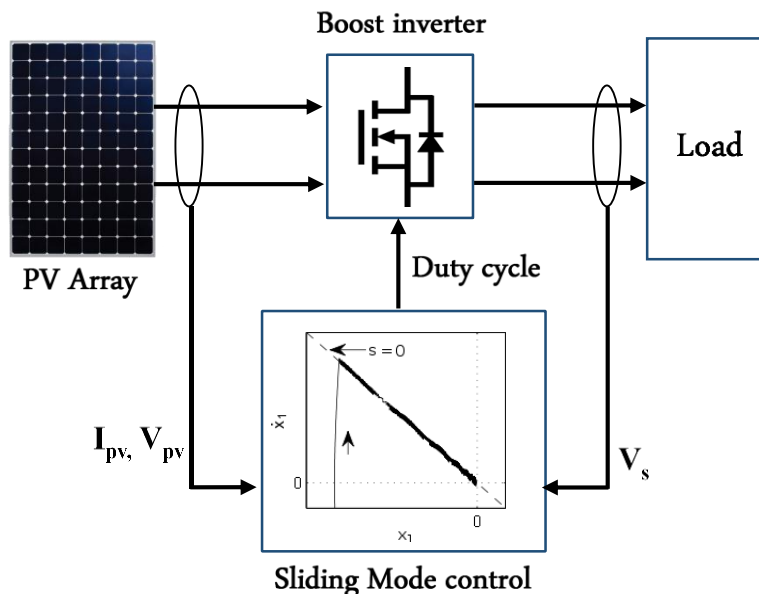


Figure 1. Structure of proposed system.

## 3. Modeling of the proposed system

### 3.1. Modeling of the photovoltaic panel

An ideal solar cell is modelled by a source of current in parallel with a diode. However, no solar cell is ideal. Therefore, two resistances are added to the model: one mounted in series and the other in parallel as it is shown in the following figure:

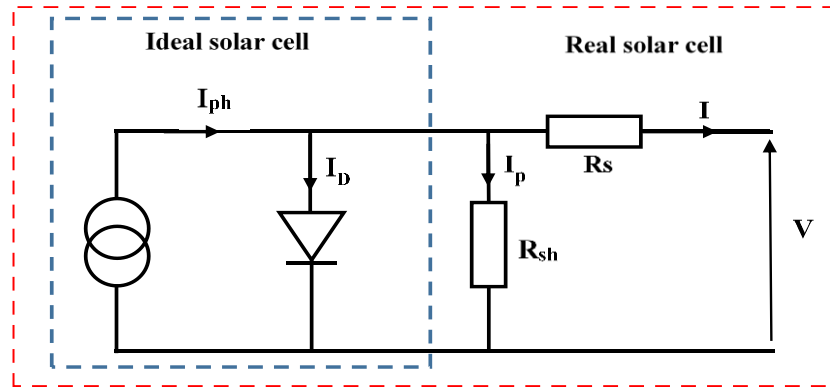


Figure 2. Electric model of solar cell.

The model above is constituted by a diode (D) characterizing the junction PN, a source of current ( $I_{ph}$ ) characterizing the photo-current, a resistance puts into series  $R_s$  representing the losses by effect Joule, and a shunt resistance  $R_{sh}$  characterizing the current of flight between the superior railing and the back contact which is generally very superior to  $R_s$ . The equation connecting the current freed by the PV cell and the tension in its borders is given the equation hereafter:

$$I = I_{ph} - I_D - I_p = I_{ph} - I_0 \left[ \exp\left(\frac{V + R_s I}{V_t}\right) - 1 \right] - \frac{V + R_s I}{R_{sh}} \quad (1)$$

Practically this equation can be simplified by considering that the resistance  $R_{sh}$  has a high value, thus the current  $I_p$  can be neglected. The equation. 1 becomes:

$$I = I_{ph} - I_0 \left[ \exp\left(\frac{V + R_s I}{V_t}\right) - 1 \right] \quad (2)$$

Therefore, the mathematical model of a PV panel, which contains  $N_p$  columns of  $N_s$  cells connected in series, is represented by the following equation:

$$I = N_p I_{ph} - N_p I_0 \left[ \exp\left(\frac{V + R_s I}{N_s V_t}\right) - 1 \right] \quad (3)$$

Where:

- The thermodynamic potential  $V_t$  :

$$V_t = \frac{KTA}{q} \quad (4)$$

- The photo-current  $I_{ph}$  :

$$I_{Ph} = [I_{scr} + K_i(T - 298)] * \frac{G}{1000} \quad (5)$$

- The current of reverse saturation of the diode:

$$I_{rs} = \left( \frac{I_{scr}}{\exp\left(\frac{qV_{oc}}{N_s kAT}\right) - 1} \right) \quad (6)$$

- The saturation current of the diode:

$$I_0 = I_{rs} \left[ \frac{T}{298} \right]^3 \exp\left[ \left( q * \frac{Eg_0}{kA} \right) \left( \frac{1}{298} - \frac{1}{T} \right) \right] \quad (7)$$

### 3.2. The boost converter modeling:

The boost converter is consisted essentially of a switch K (based on IGBT or MOSFET) and a diode D. The switch K is commanded by a pulse width modulation signal (PWM) including a fixed period  $T_d$  and a duty cycle  $\alpha$ . The conduction of both switches is complementary, when K is closed D is opened and vice-versa. to modeling the converter, we apply the Kirchoff's laws to electric circuits characterizing both sequences of functioning:

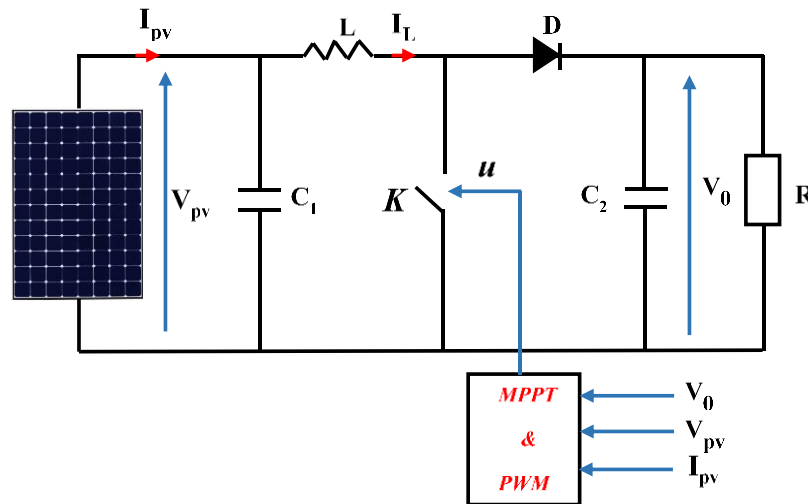


Figure 3. chain of conversion photovoltaic based of the boost inverter.

First sequence is characterized by  $u = 1$ , K is closed and D is opened. The equations that act on the converter are given as:

$$\begin{cases} \frac{di_L}{dt} = \frac{V_{pv}}{L} \\ \frac{dV_0}{dt} = -\frac{V_0}{RC_2} \end{cases} \quad (8)$$

Second sequence is characterized by  $u = 0$ , K is opened and D is closed. The system of equations that act on the converter is presented as:

$$\begin{cases} \frac{di_L}{dt} = \frac{V_{pv}}{L} - \frac{V_0}{L} \\ \frac{dV_0}{dt} = -\frac{V_0}{RC_2} + \frac{i_L}{C_2} \end{cases} \quad (9)$$

From equation (8) and (9), the boost converter mathematical model is:

$$\begin{cases} \frac{di_L}{dt} = \frac{V_{pv} - V_0}{L} + \frac{V_0}{L}.u \\ \frac{dV_0}{dt} = -\frac{V_0}{RC_2} + \frac{i_L}{C_2} - \frac{i_L}{C_2}.u \end{cases} \quad (10)$$

We take  $\mathbf{x} = [x_1 \ x_2]^T = [i_L \ V_0]^T$ , the expression (10) can be rewritten as follows:

$$\begin{cases} \frac{dx_1}{dt} = \frac{V_{pv} - x_2}{L} + \frac{x_2}{L}.u \\ \frac{dx_2}{dt} = -\frac{x_2}{RC_2} + \frac{x_1}{C_2} - \frac{x_1}{C_2}.u \end{cases} \quad (11)$$

Then:

$$\dot{\mathbf{x}} = \frac{d\mathbf{x}}{dt} = \mathbf{f}(\mathbf{x}, t) + \mathbf{g}(\mathbf{x}, t)u + \mathbf{h} \quad (12)$$

Where:

$$\mathbf{f}(\mathbf{x}, t) = \begin{bmatrix} 0 & \frac{-x_2}{L} \\ \frac{x_1}{C_2} & -\frac{x_2}{RC_2} \end{bmatrix}, \mathbf{g}(\mathbf{x}, t) = \begin{bmatrix} \frac{x_2}{L} \\ -\frac{x_1}{C_2} \end{bmatrix}, \mathbf{h} = \begin{bmatrix} \frac{V_{pv}}{L} \\ 0 \end{bmatrix}$$

### 3.3. MPPT Control strategy:

#### 3.3.1. Perturbation & Observation control:

The P&O algorithm is the most used in literature, particularly in the practical due to its simplicity of implementation. The bloc diagram of the P&O method is given in Figure.4. The panel voltage is intentionally perturbed (increased or decreased) and then the power is compared to the power obtained before the disturbance. Specifically, if the power panel is increased due to the disturbance, the next perturbed disturbance will be made in the same direction: And if the power decreases, a new perturbation is made in the opposite direction. The advantages of this method can be summarized as follows: knowledge the photovoltaic generator characteristics is not required, and it is relatively simple. Nevertheless, in steady state, the operating point oscillates around the MPP, which leads to energy losses. The MPPT is necessary to extract the maximum power from the PV module.

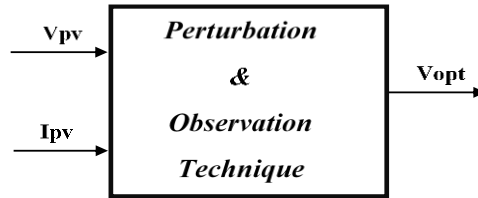


Figure. 4 Bloc diagram of Perturbation & Observation method.

### 3.3.2. Sliding mode control:

The synthesis of a sliding mode controller can be decomposed of multiple steps :

➤ **choice of the sliding surface :**

The sliding surface  $S(x)$  represents the desired dynamic behavior of system. The general equation used to determine the sliding surface which ensures the convergence of a variable towards its reference value is given by [7]:

$$S(x) = \left( \frac{\partial}{\partial t} + \lambda_x \right)^{r-1} e(x) \quad (13)$$

Where:

- $e(x)$  : is the difference between the controlled variable and its reference  $e(x) = x_{ref} - x$  .
- $\lambda_x$ : is a positive constant.
- $r$ : relative degree.

➤ **The sliding mode existence:**

The existence condition of sliding regime  $S(x) = 0$  is deduced by applying the Lyapunov's stability criterion:

$$\lim_{s \rightarrow 0} S \cdot \dot{S} < 0 \quad (14)$$

➤ **Determination of the control law:**

The sliding mode control ( $u$ ) consists of two terms: a discontinuous control term as a function of the sliding surface  $\text{sign}(u_n)$  and an equivalent control term ( $u_{eq}$ ) characterizing the dynamic of the system.

$$u = u_{eq} + u_n \quad (15)$$

Considering the system described by the following differential equation:

$$\dot{x} = f(x,t) + g(x,t)u \quad (16)$$

The derivative of the sliding surface is given by:

$$\dot{S} = \nabla S \cdot \dot{x} + \frac{\partial S}{\partial t} = \nabla S \cdot f(x,t) + \nabla S \cdot g(x,t)u + \frac{\partial S}{\partial t} \quad (17)$$

Where:  $\nabla S$  is the gradient of  $S$ .

The equivalent command which maintain the state trajectory on the sliding surface, is obtained through the resolution of equation  $\dot{S} = 0$ , and it is expressed as follows:

$$u_{eq} = -[\nabla S \cdot g(x,t)]^{-1} \left[ \nabla S \cdot f(x,t) + \frac{\partial S}{\partial t} \right] \quad (18)$$

$u_n$  is determined according to Lyapunov equation in order to guarantee the stability of the controlled system and its expression as [8]:

$$u_n = K \cdot \text{sign}(S(x)) \quad (19)$$

The gain  $K$  is chosen positive to satisfy the convergence condition  $S \cdot \dot{S} < 0$ .

## 4. Application of Sliding mode control to Track Photovoltaic System:

### 4.1. Design of the command by sliding mode control:

At the maximum power point MPP of the PV system we can have:

$$\frac{dP_{pv}}{dV_{pv}} = 0 \quad (20)$$

The first step to design the control law is the choice of the sliding surface, which can be selected using the following equation:

$$S(x) = \frac{dP_{pv}}{dV_{pv}} = I_{pv} + \frac{dI_{pv}}{dV_{pv}} \cdot V_{pv} \quad (21)$$

The figure bellow represents the Power/Voltage characteristic of photovoltaic generator at different meteorological conditions:

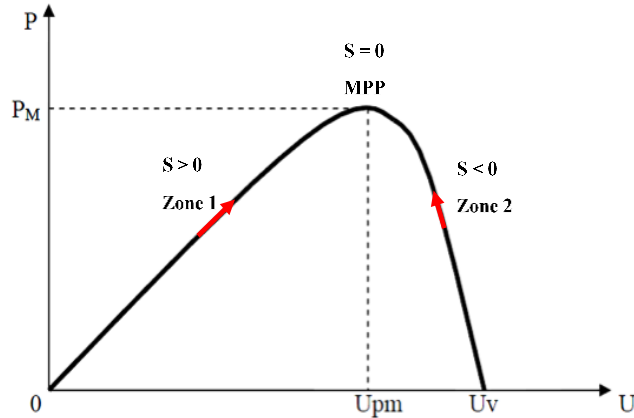


Figure 5. Typical Power-Voltage characteristic.

This characteristic can be divided of two zones separated by the point MPP ( $S(x) = 0$ ). Zone 1 is characterized by a positive slope ( $S(x) > 0$ ), and zone 2 is characterized by a negative slope ( $S(x) < 0$ ). If, for example, the operating point (OP) is in left of the MPP, The command must move it to the sliding surface by incrementing the voltage  $V_{pv}$ . If on the contrary, the OP is in right of the MPP, and the command must move the OP towards the sliding surface by decrementing the tension  $V_{pv}$ . Therefore, the adopted control is given as follows:

$$u = \begin{cases} 0 & \text{If } s(x) > 0 \\ 1 & \text{If } s(x) < 0 \end{cases} \quad (22)$$

The sliding mode control algorithm will be depicted as shown in figure 6:

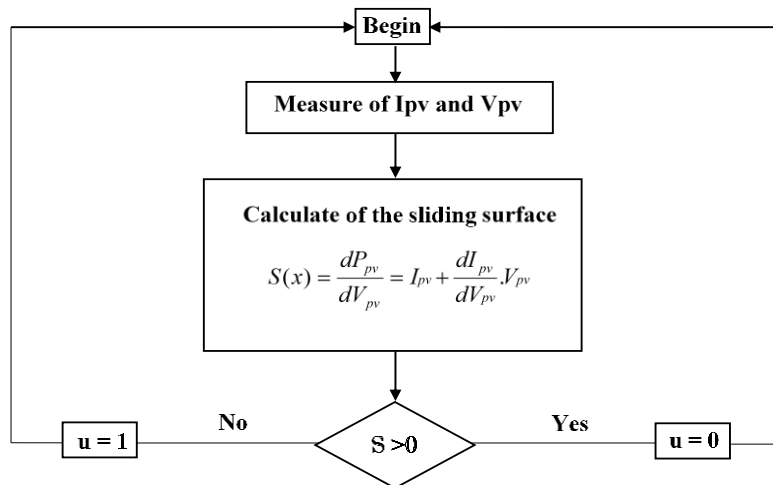


Figure 6. sliding mode control algorithm.

From equation (18), the equivalent control term  $u_{eq}$  applied to the boost is given as:

$$u_{eq} = 1 - \frac{v_{pv}}{v_0} \quad (23)$$

The equivalent command is effective only when the state trajectory of the system reached the sliding mode. The discontinuous command must be formulated to bring the trajectory on the sliding surface during the convergence mode. And it can be expressed as:

$$u_n = -k \cdot \text{sign}(S) \quad (24)$$

The global command law by sliding mode becomes:

$$u = u_{eq} - k \cdot \text{sign}(S) = 1 - \frac{v_{pv}}{v_0} - k \cdot \text{sign} \left( I_{pv} + \frac{dI_{pv}}{dv_{pv}} \cdot V_{pv} \right) \quad (25)$$

#### 4.2. Verification of the sliding mode existence:

The quadratic function of Lyapunov (V) is defined as shown in the following equation [9]:

$$V(x) = \frac{1}{2} S(x)^2 \quad (26)$$

The surface S(x) is attractive when the derivative of V is negative (attractiveness condition):

$$\dot{V}(x) = \dot{S}(x) \cdot S(x) \leq 0, \quad \forall S(x) \neq 0 \quad (27)$$

To demonstrate the sliding mode existence as presented in equation (27), the both zones illustrated in figure 5 are considered and the derivative of S(x) is calculated from equation (21):

$$\dot{S}(x) = - \left( 2 + \frac{V_{pv}}{N_s \cdot V_t} \right) \frac{N_p \cdot I_{sc}}{N_s \cdot V_t} \exp \left( \frac{V_{pv} - N_s \cdot Voc}{N_s \cdot V_t} \right) \frac{dV_{pv}}{dt} \quad (28)$$

- **Zone 1:**  $S(x) > 0$

If the OP is on the zone 1, then the voltage must be increased to reach the MPP. That means that  $\frac{dV_{pv}}{dt} > 0$ . So  $\dot{S}(x) < 0$ , and  $S(x) \cdot \dot{S}(x) < 0$ .

- **Zone 2:**  $S(x) < 0$

If the OP is on the zone 2, the voltage must be decreased to reach the MPP. That means that  $\frac{dV_{pv}}{dt} < 0$ . So  $\dot{S}(x) > 0$ , and  $S(x) \cdot \dot{S}(x) < 0$ .

We conclude that the sliding mode exists and the system is asymptotically stable whatever the operating point localization. The applied control law forces the system trajectory to converge toward the sliding surface in a finished time, and to remain it on the sliding surface until the equilibrium point.

#### 5. Simulation results:

To analyze the performance of the SMC strategy applied to the DC/DC converter, the irradiation value of 1000 W/m<sup>2</sup> and a constant temperature of 25 °C are considered in this simulation. The PV system parameters are presented in the table 1.

Table 1. PV system Parameters.

<b>PV Model : SPR-225-BLK-U</b>	
Maximum power	$P_{mpp} = 225 \text{ W}$
Voltage of maximal power	$V_{mpp} = 29.6 \text{ V}$
Current of maximal power	$I_{mpp} = 7.8 \text{ A}$
Open-circuit Voltage	$V_{oc} = 36.8 \text{ V}$
Short-circuit current	$I_{sc} = 8.47 \text{ A}$
Cell numbers	36(1×36)
Temperature coefficient of the maximum power	- 0.470%
Band-gap energy of silicon	$E_{go} = 1.1 \text{ eV}$
Temperature coefficient of the short-circuit current	$K_i = 0.0017 \text{ A/}^\circ\text{C}$
Reference temperature	$T_r = 25^\circ\text{C}$
Boltzmann Constant	$K = 1.3805 \cdot 10^{-23} \text{ J/K}$
Electron charge	$q = 1.6 \cdot 10^{-19} \text{ C}$
Diode ideality factor	$A = 1.6$
<b>DC-DC boost converter</b>	
	$C_1 = 1.2 \cdot 10^{-3} \text{ F}$
	$L = 0.5 \cdot 10^{-3} \text{ H}$
	$C_2 = 470 \cdot 10^{-6} \text{ F}$
<b>Load</b>	
	$R = 4 \ \Omega$

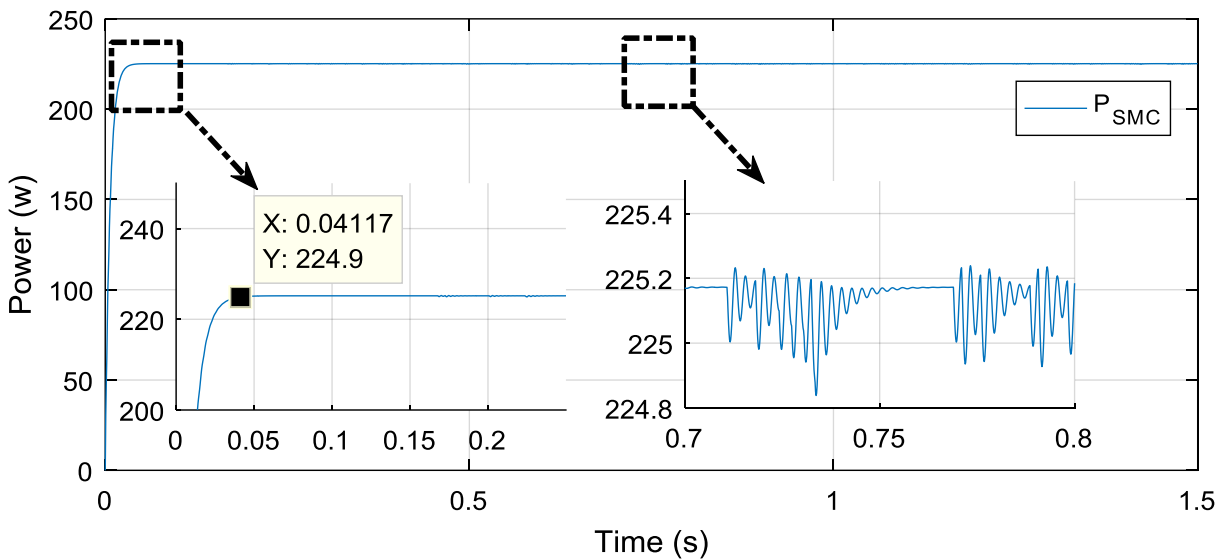


Figure7. The PV system output power .

Based on the simulation results obtained in the figure above, it is clear that the SMC presents a fast response (about 41 ms), without ripples and no overshoot.

## 6. The sliding mode control robustness

The objective of this work is to visualize the performance and the robustness of the SMC approach compared to other classical approach such as P&O method. Therefore a comparative study between P&O and SMC techniques has been done in this paper. To do this, two tests of robustness are realized by acting on the irradiation. In the first test, a constant irradiation is considered, and in the second test, a variable profile of irradiation is forced.

The PV output power obtained using P&O and SMC controller is presented in Figure.8 and Figure.9 for a constant irradiation and a variable irradiation, respectively. Each figure contains two zooms: zoom in the left illustrate the response time and zoom in the right illustrate the oscillations around the MPP in the steady state.

Under a constant irradiation as illustrate in Figure.8, the SMC and P&O follow the PPM with a different response time (41 ms for SMC and 111 ms for P&O). In addition, the P&O presents a significant oscillations around the MPP (between 235.6 W and 198.3 W).

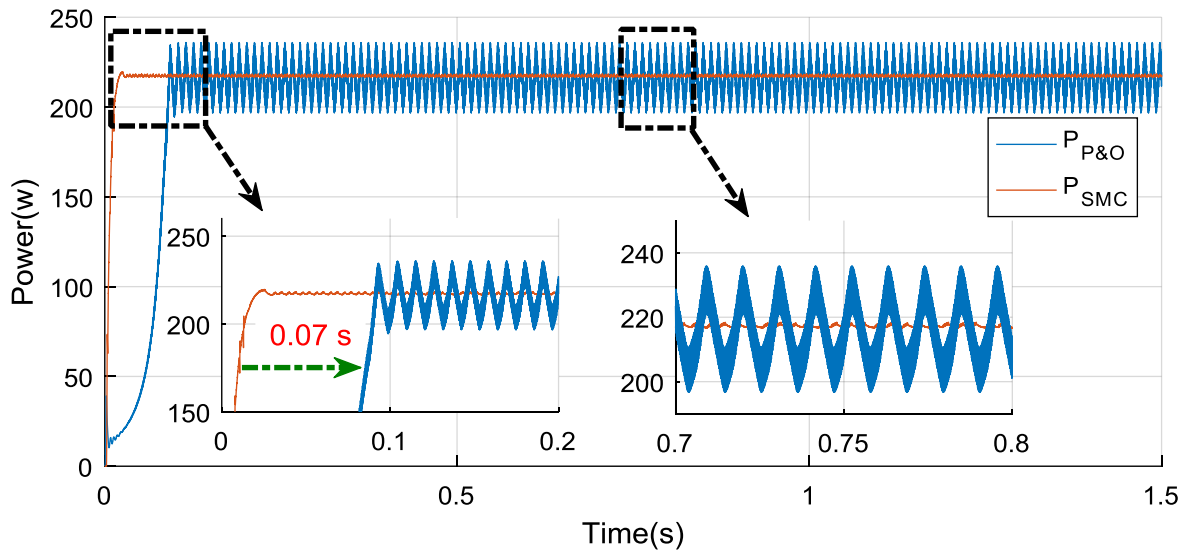


Figure.8. Comparison of the PV system output power between SMC and P&O control under a constant irradiation.

Under a variable irradiation (Figure.9) there are the same response time and almost the same oscillations around the MPP. Also, we can see that with a variation of irradiation, the P&O losses about 3 joule of the energy with respect to the SMC.

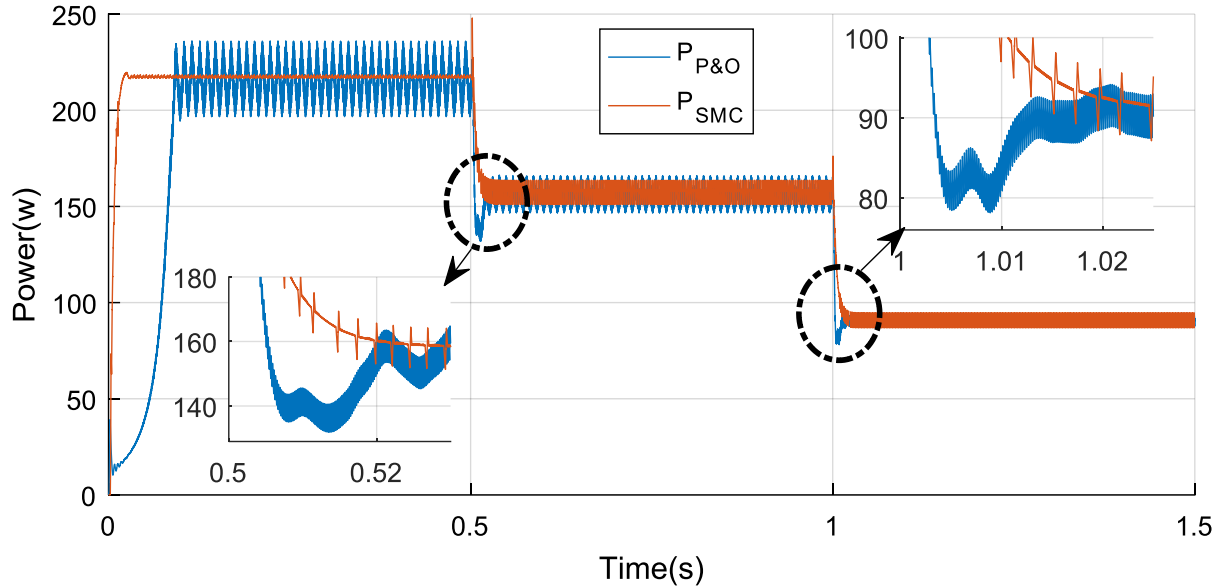


Figure.9.Comparison of the PV system output power between SMC and P&O control under a variable irradiation.

All results mentioned previously are summarized in the following tables:

Table 2. Comparison results under a constant irradiation.

Command technique	P&O	SMC
Response time	111 ms	41 ms
Oscillation amplitude	37.3 W	0.043 W

Table 3. Comparison results under a variable irradiation.

Command technique	P&O	SMC
Response times	111 ms	41 ms
Losses energy when there is a change of irradiation	3 J	0 J

From these results, it can be concluded easily that the SMC has enormous advantages compared to other MPPT-techniques such as the P&O method, it provides to achieve the steady state in a very short time of the milliseconds order, with a reduced oscillation.

## 7. Conclusion:

The work presented in this paper consist on the optimization study of an Autonomous PV solar system. In order to extract the maximum PV power, an approach based on sliding mode has been proposed. The validation of this method is performed by simulation under the Simulink/Matlab software in a chain based on a boost converter. The simulation results clearly show that the proposed method is effective for MPP tracking research regardless the sun climatic conditions. In addition, it is able to put the OP on the MPP quickly, contrary to other methods that require more time. The obtained results confirm those theoretically predicted. Therefore, it can be concluded that the proposed control strategy can be considered as an interesting solution in the field of photovoltaic systems control.

## References

- [1] S. Ould-Amrouche, D. Rekioua , A. Hamidat, Modelling photovoltaic water pumping systems and evaluation of their CO2 emissions mitigation potential, *Applied Energy* 87 (2010) 3451–3459.
- [2] A. Anurag, S. Bal, S. Sourav, and M. Nanda, “A review of maximum power-point tracking techniques for photovoltaic systems,” *Int. J. Sustain. Energy*, vol. 35, no. 5, pp. 478–501, 2016.
- [3] M. M. Shebani, T. Iqbal, and J. E. Quaicoe, “Comparing bisection numerical algorithm with fractional short circuit current and open circuit voltage methods for MPPT photovoltaic systems,” in *2016 IEEE Electrical Power and Energy Conference (EPEC)*, 2016, pp. 1–5.
- [4] Ahmed Sher ,H., Murtaza ,A. F., Noman ,A., Addoweesh ,K. E., Al-Haddad ,K., and Chiaberge ,M. ‘A New Sensorless Hybrid MPPT Algorithm Based on Fractional Short-Circuit Current Measurement and P&O MPPT’, *IEEE Transactions on sustainable energy*, pp 1-9, 2015.
- [5] Al-Shetwi, A.Q., Muhamad Zahim, S., 2016. Modeling and simulation of photovoltaic module with enhanced perturb and observe MPPT algorithm using Matlab/Simulink. *ARNP J. Eng. Appl. Sci.* 11 (2016), 12033–12038.
- [6] D. Verma, S. Nema, A. M. Shandilya, and S. K. Dash, “Maximum power point tracking (MPPT) techniques: Recapitulation in solar photovoltaic systems,” *Renew. Sustain. Energy Rev.*, vol. 54, pp. 1018–1034, 2016.
- [7] W. Lu, C. Li, and C. Xu, “Sliding mode control of a shunt hybrid active power filter based on the inverse system method,” *Int. J. Electr. Power Energy Syst.*, vol. 57, pp. 39–48, 2014.
- [8] H. Komurcugil, “Adaptive terminal sliding-mode control strategy for DC–DC buck converters”, *ISA Transactions* vol.51, 2012, pp.673-681.
- [9] N. Khemiri, A. Khedher, and M. F. Mimouni, “A sliding mode control approach applied to a photovoltaic system operated in MPPT,” *10th Int. Multi-Conferences Syst. Signals Devices* 2013, pp. 1–6, 2013.

## Biographies



**Mohamed Mansori** was born in Errachidia, Morocco, in 1994. He received the M.S degree in Electrical Engineering in 2017 from Mohammed V University, ENSET, Rabat-Morocco. Currently he is working toward PhD in the Electrical Engineering Research Laboratory LRGE, since 2017. His research interests are related to renewable energies. His current activities includes control strategies of photovoltaic energy conversion system, and energy storage technologies.



**Malika Zazi** is currently a professor and university research professor at the electrical engineering department of ENSET, Mohamed V University, Rabat-Morocco. In 2006, He received her PhD degree from Mohammadia engineering school (EMI), Rabat-Morocco. Her current research interests include renewable energy, motor drives and power system. Maliza zazi is Assistant Director for Pedagogical Affairs at ENSET-Rabat and a Founding Member of the University Entrepreneurship Center of Mohamed V University.